Parameter Estimation of Linear FM Scatterometer Pulses Received by the SeaWinds Calibration Ground Station

Spencer S. Haycock
Microwave Earth Remote Sensing Laboratory
Brigham Young University
459 Clyde Building
Provo, Utah 84602

***Abstract*— An overview of the purpose and operation of the SeaWinds Calibration Ground Station is presented. Several possible signal measurement techniques are analyzed in order to create a feasible signal metrology for the NASA SeaWinds instrument. This analysis helps to advance the level to which future scatterometer instruments may be calibrated, providing the potential for a more accurate scatterometer data product.**

I. Introduction: Estimation of Scatterometer Signal Parameters and Its Application

A scatterometer is an orbiting radar that allows scientists to study the Earth's environment on a global scale. It can be used to measure properties of both the atmosphere and the Earth's surface. For example, it can measure wind velocity to understand weather patterns and detect climatic changes, observe polar sea ice (track icebergs), and estimate surface moisture or vegetation to detect drought or deforestation. In order to produce accurate estimates of these environmental factors, the scatterometer must be precisely calibrated.

The SeaWinds Calibration Ground Station (CGS) was developed by NASA Jet Propulsion Laboratory (JPL) to receive SeaWinds transmissions, allowing passive measurement of the signal characteristics in post processing. Independent characterization of these transmissions has allowed JPL to verify correct operation of the SeaWinds scatterometer, increasing the validity of their environmental measurements. In this paper, the SeaWinds Calibration Ground Station is presented and parametric estimation methods are introduced as possible ways to precisely measure key characteristics of the scatterometer transmissions.

II. The SeaWinds Scatterometer (Transmitter)

The SeaWinds scatterometer is located onboard the QuikSCAT satellite in an 803-km sun-synchronous low earth orbit. The scatterometer transmits electromagnetic pulses to the Earth's surface, from which the backscatter is received and observed in order to indirectly obtain environmental measurements. QuikSCAT's orbit allows SeaWinds to illuminate more than 90% of the Earth's surface in 24 hours, usually passing over the BYU Microwave Earth Remote Sensing Laboratory (Provo, Utah) twice daily.

SeaWinds transmits pulses at a chirped carrier frequency centered at $f_0 = 13.402$ GHz. This frequency was also used in the NSCAT project and was chosen because it has been found that frequencies near 13.4 GHz are "sensitive to capillary waves on the ocean surface induced by local winds" [1].

Linear FM chirped pulses are transmitted from two alternating antenna beams. The transmitted pulses, the analysis of which is the main focus of this paper, are linear FM chirped. The outer antenna is elevated 46° from nadir and transmits vertically polarized pulses; the inner antenna is elevated at 40° and transmits pulses that are horizontally polarized [1]. The pulse width $\tau = 1.5$ ms and nominal pulse repetition interval (PRI) of 5.4 ms were based on "spacecraft altitude and antenna scanning geometry" and were chosen to "produce a beam pattern which covers the scan swath without gaps" [1]. Note that since the transmitted pulses successively alternate between the inner and outer beams, the effective PRI of each beam is approximately 10.8 ms.

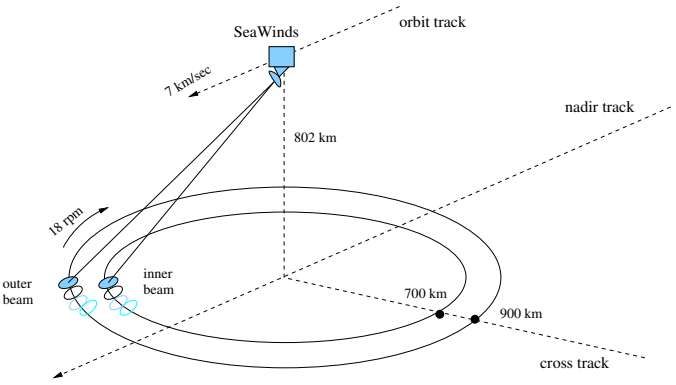

Fig. 1. SeaWinds ground track [2].

The antenna rotates at 18 rpm, tracing out a helical pattern on the Earth's surface (Fig. 1). As the antenna rotates, the two-way Doppler shift observed by SeaWinds from echoed pulses varies as a cosine of amplitude 480 kHz (430 kHz) for the outer beam (inner beam) [1]. Commanded Doppler compensation is used to precompensate the carrier frequency f_0 for the anticipated Doppler effect expected in echoed pulses, so that no net Doppler shift results (within 10 kHz) [3]. This allows the SeaWinds receiver to operate with a fixed

TABLE I
SEAWINDS KEY PARAMETERS [1] [3]

Parameter	Value
Instrument frequency	13.402±0.0005 GHz
Chirp rate	-250.73 kHz/ms
Transmit pulse width	1.5 ms
Nominal PRI	5.4 ms
Doppler tracking range	±600 kHz
Antenna spin rate	18 rpm
Antenna peak sidelobe	≤ -15 dB
Outer beam	
Look angle	46° from nadir
3-dB beamwidth	1.4°(el) x 1.7°(az)
Range Delay	8.3 ms
Inner Beam	
Look angle	40° from nadir
3-dB beamwidth	1.6°(el) x 1.8°(az)
Range Delay	7.3 ms

Fig. 2. Receiver of the SeaWinds Calibration Ground Station. Tubes pump cool air into the radome and protect sensitive cables connected to computers below.

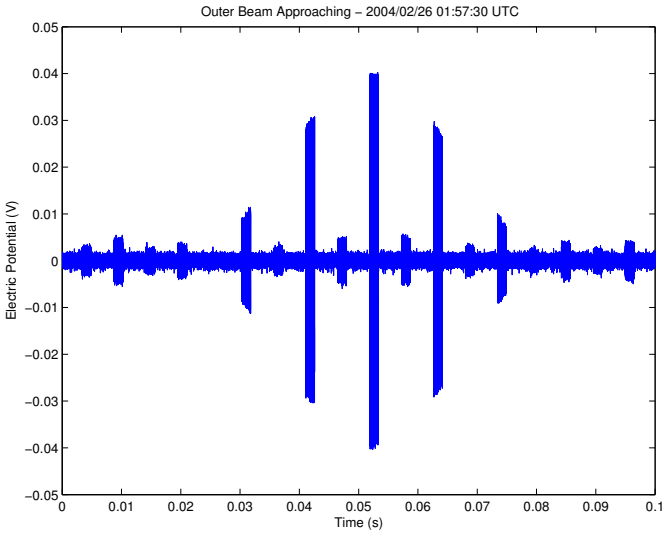

Fig. 3. The outer beam of SeaWinds sweeps across the main lobe of the CGS receiver during a flyby over Provo, Utah.

frequency response intended for the echo returns [1]. In order to account for orbital geometry, the commanded Doppler is parameterized by a lookup table as QuikSCAT traverses its orbit. The commanded Doppler consists of a cosine function with phase, amplitude, and bias parameters for 256 equally-spaced temporal orbit steps [1].

III. THE CALIBRATION GROUND STATION (RECEIVER)

The CGS (Fig. 2) was previously located in White Sands, New Mexico, in order to calibrate the scatterometer onboard the QuikSCAT satellite (launched in June 1999). It was acquired by the BYU Microwave Earth Remote Sensing (MERS) Laboratory in March 2002 in order to continue monitoring SeaWinds on QuikSCAT and to observe transmissions from the SeaWinds scatterometer onboard the ADEOS-II satellite, launched in December 2002. However, the ADEOS-II satellite suddenly lost power in October 2003 so that only SeaWinds on QuikSCAT is currently observed by the CGS.

The CGS, positioned on the roof of the Clyde Building on BYU campus, regularly receives SeaWinds transmissions. In order to successfully receive a signal, the computer-controlled pedestal is programmed to point the receiving antenna at SeaWinds during each flyby. The CGS antenna is held fixed during each beam capture to reduce jitter. This is possible due to the fact that the CGS antenna has a wide main lobe. During each flyby, the CGS is illuminated for several brief intervals called sweeps (Fig. 3). Pulses with adequate SNR within these sweeps are detected, from which key signal parameters are extracted during post processing.

A. Operation and Maintenance

Usually, only ten seconds of SeaWinds transmissions (corresponding to three beam sweeps) are sampled for the pass of each beam over the CGS, for a total of 40 s of received signal. These 10-s captures are stored in successive 100-ms ".raw" files for offline processing. Each ".raw" file contains a 1024-byte header which reveals basic sampling information, including start time, beam description, and first and second-order signal statistics. Depending on computer hardware restrictions, these files can be linked together to form one large data capture.

Meticulous hardware and software maintenance of the CGS has been required to sustain the CGS and archive its data for post processing. Over the course of the project, the following tasks have been completed:

1) Converted the CGS to receive SeaWinds transmissions from QuikSCAT after the failure of SeaWinds on ADEOS-II.
2) Maintained CGS hardware and software to correctly capture SeaWinds transmissions.
3) Archived captured data on a daily basis; backed up these archives to CD-R.
4) Researched and developed parameter estimation methods to characterize received transmissions by extracting

the following parameters:

- Signal power
- Pulse duration
- Pulse repetition interval (PRI)
- Pulse bandwidth
- Chirprate
- Doppler shift
- Doppler compensation
- Phase consistency (coherency)

B. Sampling Scheme

The receiving antenna is a circularly polarized corrugated horn antenna. The CGS receiver is a double conversion superheterodyne that consists of two parts: the front end is located in an insulated metal box mounted on the pedestal within the radome, while the rest is cascaded via coaxial cable to a component on the computer racks. The signal is folded to 35 MHz, sampled, and decimated to yield an effective 5.1875 MHz sample rate. The undersampling in this process leads to aliasing which results in a reversal in the frequency spectrum (Fig. 4), where the SeaWinds linear FM downchirp is perceived as an upchirp.

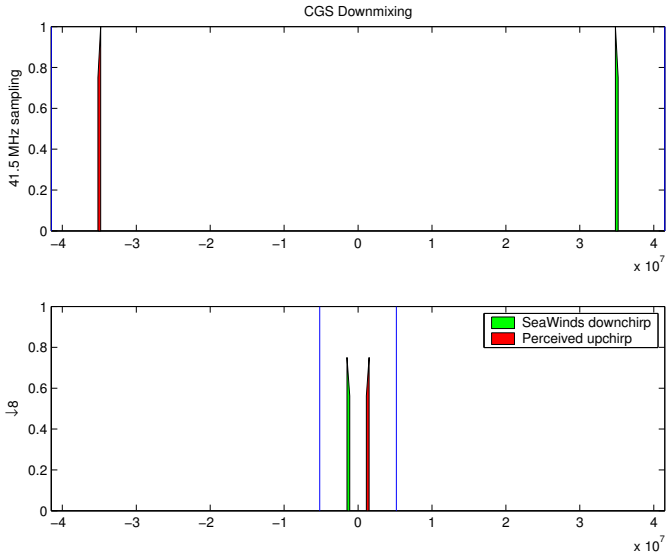

Fig. 4. CGS downmixing scheme.

IV. Pulse Detection

SeaWinds pulses are linear frequency-modulated (LFM) at $\mu = -250.73$ kHz/ms. The pulses have duration $\tau \approx 1.5$ ms, yielding a pulse bandwidth of $B \approx 375$ kHz. The CGS receives pulses at various SNR depending on the alignment of the SeaWinds and CGS antenna beams. Parameter estimation of these pulses requires that the pulses be found under both high- and low-SNR conditions. A brief explanation of linear FM waveforms is given, followed by techniques to find their location in noise.

A. Linear FM Waveforms

LFM waveforms are a subclass of polynomial-phase signals of the form

$$x(t) = \mathfrak{Re}\left\{Ae^{j\phi(t)}\right\} \tag{1}$$

where the instantaneous phase of order p is defined as $\phi(t) = \sum_{i=0}^{p} a_i t^i$. The instantaneous frequency of the waveform may be obtained by applying a time derivative to the instantaneous phase and converting from radians to Hz, yielding

$$f(t) = \frac{1}{2\pi}\frac{d}{dt}\phi(t). \tag{2}$$

For an LFM waveform,

$$\phi(t) = 2\pi\left(\frac{\mu}{2}t^2 + f_0 t\right) + \phi_0 \tag{3}$$

with chirp rate μ (Hz), frequency f_0 (Hz), and phase ϕ_0 (rad). Notice that the instantaneous frequency $f(t) = \mu t + f_0$ of the LFM waveform is swept linearly in time.

B. Determination of Temporal Pulse Location

In order to extract pulse parameters, pulses must be located in time. Ambient noise complicates this process to the point of making the problem nontrivial. However, once one pulse is located, the temporal locations of many other pulses within its vicinity may be estimated by knowing the approximate PRI *a priori*. A high-SNR pulse may be chosen as a reference point from which the temporal regions of other pulses may be initially predicted (assuming the actual PRI deviates only slightly from the *a priori* PRI) and then accurately located.

Recall that ".raw" files are equipped with headers that contain statistical information about the data samples. To quickly locate a pulse with relatively high SNR within a SeaWinds pass, the ".raw" file with maximum signal variance is selected since variance may be used as a metric of average power [4]. Next, the sample of maximum amplitude within this interval is identified, which is assumed to lie within the pulse of maximum power within the file under consideration. Since we know the approximate duration of each pulse, a time interval may be derived where the boundaries of the pulse must lie in relation to the lone sample.

1) Definition of Temporal Pulse Boundary: Determining the boundaries of chirped pulses is somewhat arbitrary since there is no precise definition of the pulse boundary in the time or frequency domain. Therefore, we must pick a definition to be consistent. It may be simple to identify the boundaries of a pulse in a plot of signal power; in other cases, noise may render a pulse undetectable. Thus, defining the temporal boundary of a pulse is complicated by the existence of the noise floor in the received signal. Since the noise floor always exists, simply defining the pulse to start wherever the signal begins to have nonzero amplitude is impossible. Thus, the edge of the noisy pulse must be defined in some other way.

Possible definitions of the pulse boundary may be made with respect to signal power or frequency. For example, the pulse may be defined to start corresponding to the interval over which the average power per sample is maximized, or where the zero-crossings of the waveform start to be evenly spaced

in time. Since the resolution of defining the pulse boundary with respect to power is not limited by the wavelength of the received signal, it is a more logical choice.

2) Incoherent Matched Filtering: If the duration of the pulse is known but its location in a temporal region is unknown, it may be found by convolving the signal power with a boxcar (rectangle of unity height) of the same length as the pulse. The resulting apex (Fig. 5) reveals the sample corresponding to the trailing edge of the pulse. Although easy to implement, this method requires *a priori* knowledge of the pulse length, which may vary slightly from what it is assumed to be. However, the duration may be estimated by observing boundaries of pulses with high SNR near the pulse under consideration. Obviously, this could lead to inaccurate estimates of the locations of the leading and trailing edges of the pulse.

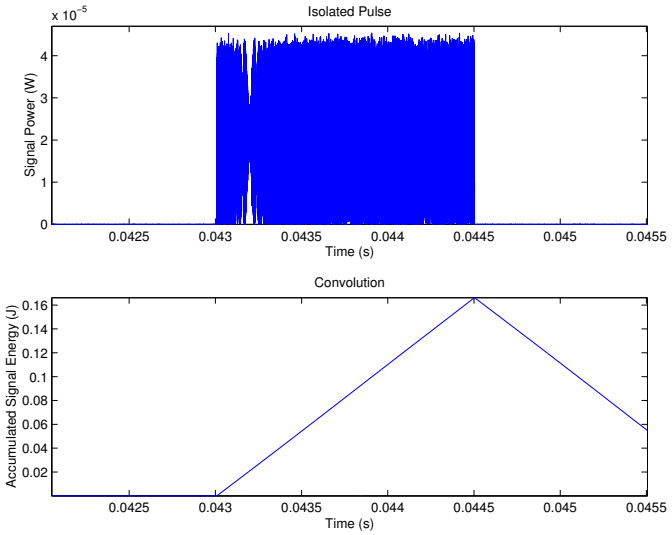

Fig. 5. Computation of pulse boundaries using incoherent matched filtering.

3) Integrated Signal Power: Alternatively, if the duration of a pulse is unknown, the pulse may be found by observing the average power per sample as a function of the proposed leading and trailing edges of the pulse. Notice how the average power per sample is maximized (Fig. 6) as the proposed leading edge τ crosses the true leading edge of the pulse. If the area of integration encompasses the entire pulse, the start of the pulse is indicated by maximizing the function of average power per sample with respect to the placement of the leading edge of the pulse. However, in low-SNR cases it may be difficult to resolve this point.

V. Matched Filter Bank

A matched filter correlates a received signal with a signal we wish to detect (Fig. 7), providing the maximum possible output SNR when the received signal contains white Gaussian noise [5]. This inherently requires *a priori* knowledge of signal parameters such as chirprate and initial frequency; otherwise, the matched filter will not provide an optimal output SNR. Hence, its purpose is not intended to measure signal parameters, but to detect known signals. However, estimation

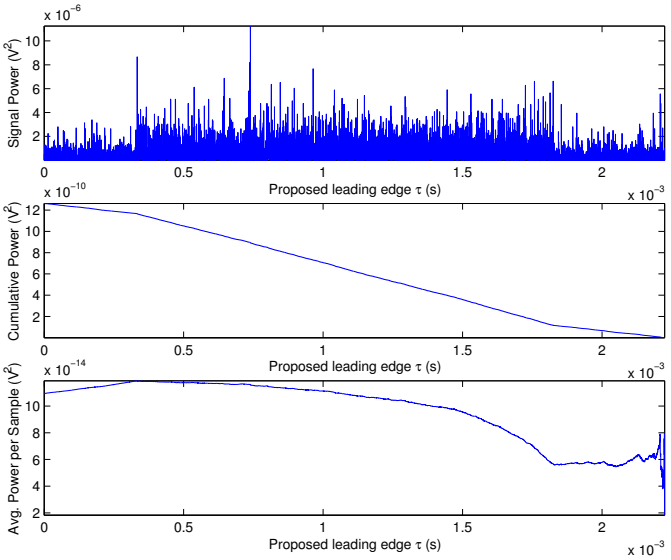

Fig. 6. Computation of pulse boundaries using integrated power per sample.

may be implemented by using a bank of matched filters over a range of signal parameters.

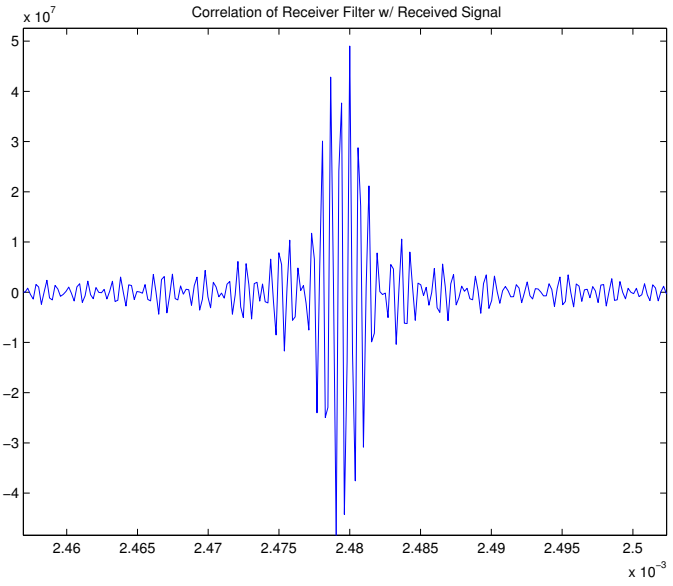

Fig. 7. Output of matched filter: cross correlation of filter with received signal.

VI. Regression on Unwrapped Signal Phase

Under high-SNR conditions, several signal parameters may be estimated by applying a least-squares approximation to the unwrapped signal phase [6]. First, the instantaneous phase $\phi(t)$ of the signal $e^{j\phi(t)}$ is unwrapped. In this case, quadratic regression is applied to $\phi(t) = 2\pi\left(\frac{\mu}{2}t^2 + f_0 t\right) + \phi_0$, revealing the signal parameters: chirp rate μ, frequency f_0, and phase ϕ_0. However, this technique is complicated by the fact that it is difficult to perform phase unwrapping at low SNR, due to noise. An equivalent technique is to apply a least-squares approximation to the zero-crossing times of the signal. Notice

that the coefficients of t in the argument of the cosine may easily be found by setting the argument equal to odd multiples of $\frac{\pi}{2}$, which correspond to the zero-crossings of a cosine:

$$\phi(t) = n\frac{\pi}{2}, \tag{4}$$

where n is odd. A linear system may then be solved for the coefficients of the quadratic phase.

To obtain the zero-crossing times, coupled samples that are opposite in sign must be found (since a zero-crossing must occur somewhere between these two samples). Linear interpolation may be justified by observing the linear portion of the cosine function near the zero-crossings of the waveform. Using $y = mt + b = 0$, where y is the waveform amplitude, m is the linearly interpolated slope, t is the time, and b is the amplitude of the sample we are referencing from, the linearly interpolated zero-crossing of the waveform occurs at $t = -b/m$.

Accuracy may be increased by upsampling the waveform to a higher sampling rate. This allows the estimation of zero crossings to be more accurate by linearly interpolating between samples that are closer to the linear portion of the sinusoidal waveform.

VII. Joint Time-Frequency Transforms

Time-frequency distributions (TFDs) are joint density functions of time and frequency that allow the observation of a time-changing signal spectrum.

A. Spectrogram

The Short-Time Fourier Transform (STFT) is one of the most widely known time-frequency transforms. It is simply the result of the Fourier transform on successive windowed portions of data. The moving window limits the interval over which the Fourier transforms are taken, effectively dividing the signal into time segments so that frequency change may be observed over time. The window function $w(t)$ thus emphasizes a specific time interval of the signal, suppressing the signal outside of this interval. The STFT is defined as

$$S_x(t,f) = \frac{1}{2\pi}\int x(\tau)w(\tau - t)e^{-j2\pi f\tau}d\tau \tag{5}$$

By sliding the window over time t, a plot of signal energy is created over the time-frequency plane. It can be interpreted as the projection of the signal onto a set of bases parameterized by time and frequency. Since the bases are of finite time duration, the varying signal spectrum may be observed as a function of time [5].

The squared STFT results in the spectrogram, a time-varying analysis of the signal spectrum. Disadvantages of the spectrogram include lack of finite support and localization tradeoff between time and frequency [7].

B. Wigner Distribution (WD)

The Wigner Distribution (WD), also known as the Wigner-Ville Distribution (WVD) when using the analytic signal, is a popular TFD (Fig. 8) well-known for its high resolution and convenient properties. Since a window is not used in the WD, its resolution is not impeded by the limitations introduced by a window function [8]. The WD is defined as

$$W_x(t,f) = \int x(t + \frac{\tau}{2})x^*(t - \frac{\tau}{2})e^{-j2\pi f\tau}d\tau. \tag{6}$$

which is the Fourier transform of the instantaneous autocorrelation function $R_x(t,\tau) = x(t + \frac{\tau}{2})x^*(t - \frac{\tau}{2})$ [9]. Just as the Fourier transform is a projection of a signal onto a basis of complex exponentials equally spaced in frequency, the Wigner distribution is a signal projection onto autocorrelation functions of the signal.

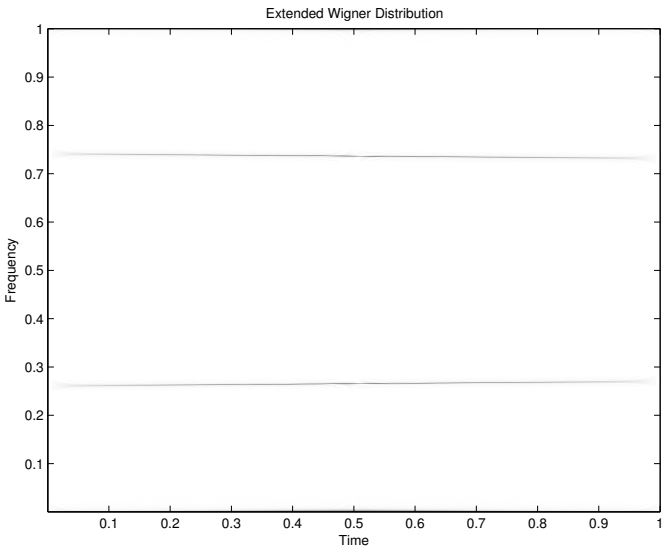

Fig. 8. Extended Discrete-Time Wigner Distribution (EDTWD) of a linear FM chirp.

Attempts to create a discrete-time version of the Wigner Distribution have resulted in implementations that suffer from inherent aliasing problems. To overcome aliasing, the signal must be sampled at twice the Nyquist rate or the analytic signal (which eliminates the existence of negative frequencies in the frequency domain) must be used. A popular discrete-time implementation is known as the Discrete-Time Wigner Distribution (DTWD):

$$W_x(n,f) = 2\sum_k x(n+k)x^*(n-k)e^{-j4\pi fk}. \tag{7}$$

C. Radon Transform of the WD

Maximum likelihood (ML) detection of a linear FM signal in white noise is accomplished by integrating along all lines of the WD [10], [11]. Detection of a linear FM signal is declared if the maximum value of integration exceeds a specified threshold. This line integration is also known as the Radon transform, an advantage of which is the restriction of the line integration to specific regions of the time-frequency plane, easing the computational burden of detection [11].

The Radon Transform of a two-dimensional function $w(x,y)$ is

$$\Re\{w(x,y)\} = \int w(r\cos(\phi) - s\sin(\phi), r\sin(\phi) + s\cos(\phi))ds \tag{8}$$

where r and s are the x and y axes rotated counterclockwise by ϕ radians [10]. A convenient property of the Radon Transform of the WD is that it can be efficiently implemented via a dechirping algorithm that does not require the direct calculation of the WD.

D. Radon-Wigner Transform

The Radon Transform of the WD may be written as

$$\mathfrak{R}_{W_x}(r,\phi) = \mathfrak{R}\{W_x(t,f)\} \quad (9)$$

$$= \int W_x(t, f_0+\mu t)dt\Big|_{f_0=r/2\pi\sin(\phi)}^{\mu=-\cot(\phi)/2\pi}. \quad (10)$$

and may be equated to dechirping in discrete-time as [10]:

$$\sum_n W_x^e(n, f_0+\mu n) = \left|\frac{1}{\sqrt{N}}\sum_{n=0}^{N-1} x(n)e^{-j2\pi(\frac{\mu}{2}n^2+f_0 n)}\right|^2 \quad (11)$$

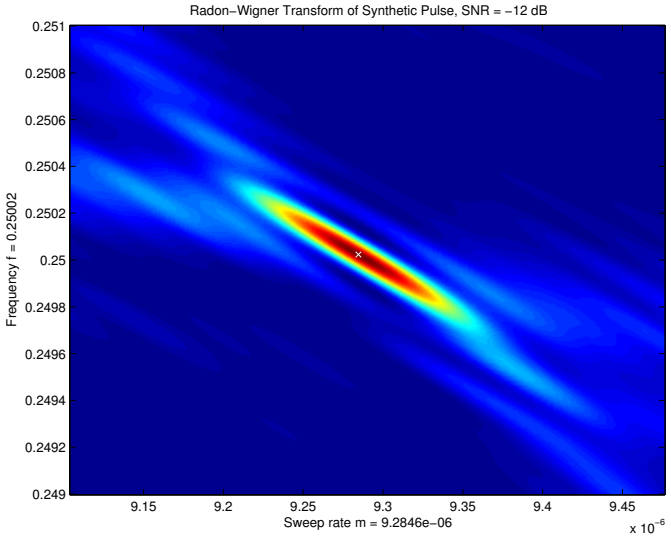

Fig. 9. Radon-Wigner Transform of a linear FM waveform.

E. SNR Considerations

Since a low SNR leads to less accurate calculations (due to high levels of noise), we discriminate high-SNR pulses from those of low SNR. Before calculating SNR, the level of observed ambient noise must be computed. First, an interval of the CGS capture must be selected that does not contain any pulses. The mean signal power in this interval is computed to estimate the average power of the noise floor. To obtain the SNR for each pulse, the noise floor is subtracted from the average power of the noisy signal to obtain an estimate of the actual signal power in each pulse, from which the noise power is divided to obtain the SNR.

F. Doppler Analysis

After obtaining the parameter estimates of several successive pulses as SeaWinds approaches and recedes from the CGS, the Doppler shift may be observed by locating pulses in time, obtaining frequency estimates, and interpolating Doppler shift where low-SNR pulses or an absence of pulses occur.

Recall that the Doppler compensation cancels the two-way Doppler effect in the RCS backscatter. Hence, the CGS observes the sum of a one-way Doppler shift (caused by the QuikSCAT satellite approaching or receding from the CGS) and SeaWinds' two-way Doppler compensation. This causes an apparent sinusoidal oscillation in the observed frequencies of consecutive pulses (Fig. 10).

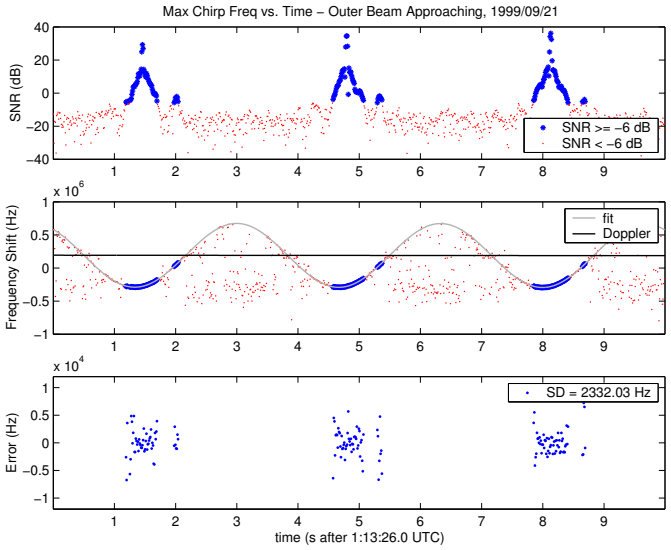

Fig. 10. Outer beam approaching

VIII. Future Research

This work is still in progress. Although several methods exist to estimate parameters of linear FM waveforms, the accuracy of such methods needs to be evaluated. Once this is done, decision regions may be created which choose algorithms according to appropriate SNR. Additionally, the effects of nonconstant signal amplitude, which occcurs during sweeps of the SeaWinds scatterometers will be considered.

IX. Conclusion

The SeaWinds Calibration Ground Station is essential to verify correct operation of the SeaWinds scatterometer. This verification helps NASA JPL to improve the accuracy of their data products, advancing the quality of their environmental estimates, thereby furthering the ability to understand the Earth's environment.

References

[1] C. Wu, Y. Liu, K. H. Kellogg, K. S. Pak, and R. L. Glenister, "Design and calibration of the Seawinds scatterometer," *IEEE Trans. Aerosp. Electron. Syst.*, vol. 39, pp. 94–109, Jan. 2003.

[2] A. Anderson, "Analysis and usage of the Quikscat Calibration Ground Station," Master's thesis, Brigham Young University, Provo, Utah, 2001.

[3] R. D. Crowley, "Hardware design overview of a satellite scatterometer," in *Southeastcon '98*, Apr. 1998, pp. 244–247.

[4] J. T. Adams and J. P. Lux, "Ground calibration of an orbiting spacecraft transmitter," in *Aerospace Conference Proceedings, 2000 IEEE*, vol. 5, Mar. 2000, pp. 37–49.

[5] V. C. Chen, *Time-frequency transforms for radar imaging and signal analysis*. Boston: Artech House, 2002.
[6] P. M. Djurić and S. M. Kay, "Parameter estimation of chirp signals," *IEEE Trans. Acoust., Speech, Signal Processing*, vol. 38, pp. 2118–2126, Dec. 1990.
[7] L. Cohen, *Time-Frequency Analysis*. Englewood Cliffs, NJ: Prentice Hall PTR, 1995.
[8] F. Hlawatsch, *Time-frequency analysis and synthesis of linear signal spaces: time-frequency filters, signal detection and estimation, and range-doppler estimation*. Boston: Kluwer Academic Publishers, 1998.
[9] B. Boashash, "Heuristic formulation of time-frequency distributions," in *Time Frequency Signal Analysis and Processing: A Comprehensive Reference*, B. Boashash, Ed. Amsterdam ; Boston: Elsevier, 2003.
[10] J. C. Wood and D. T. Barry, "Radon transformation of time-frequency distributions for analysis of multicomponent signals," *IEEE Trans. Signal Processing*, vol. 42, pp. 3166–3177, Nov. 1994.
[11] S. Kay and G. F. Boudreaux-Bartels, "On the optimality of the wigner distribution for detection," in *IEEE International Conference on Acoustics, Speech, and Signal Processing 1985*, vol. 10, Apr. 1985, pp. 1017–1020.